

Supporting Information for

Reaction Mechanism of Zika Virus NS2B/NS3 Serine Protease Inhibition by Dipeptidyl Aldehyde: A QM/MM Study

Bodee Nutho,¹ Adrian J. Mulholland,^{2*} and Thanyada Rungrotmongkol^{3,4*}

¹Program in Biotechnology, Faculty of Science, Chulalongkorn University, Bangkok 10330, Thailand

²Centre for Computational Chemistry, School of Chemistry, University of Bristol, Bristol BS8 1TS, UK

³Structural and Computational Biology Research Unit, Department of Biochemistry, Faculty of Science, Chulalongkorn University, Bangkok 10330, Thailand

⁴Ph.D. Program in Bioinformatics and Computational Biology, Faculty of Science, Chulalongkorn University, Bangkok 10330, Thailand

*Corresponding authors. TR Fax: +66 2 218-5418; Tel: +66 2 218-5426, AJM Fax: +44(0)117-925-0612; Tel: +44(0)-117-928-9097

E-mail address: thanyada.r@chula.ac.th, adrian.mulholland@bristol.ac.uk

Table of Contents

Fig. S1.....	3
Fig. S2.....	4
Fig. S3.....	5
Fig. S4.....	6
Fig. S5.....	7
Fig. S6.....	8
Fig. S7.....	9
Fig. S8.....	10
Fig. S9.....	11
Fig. S10.....	12

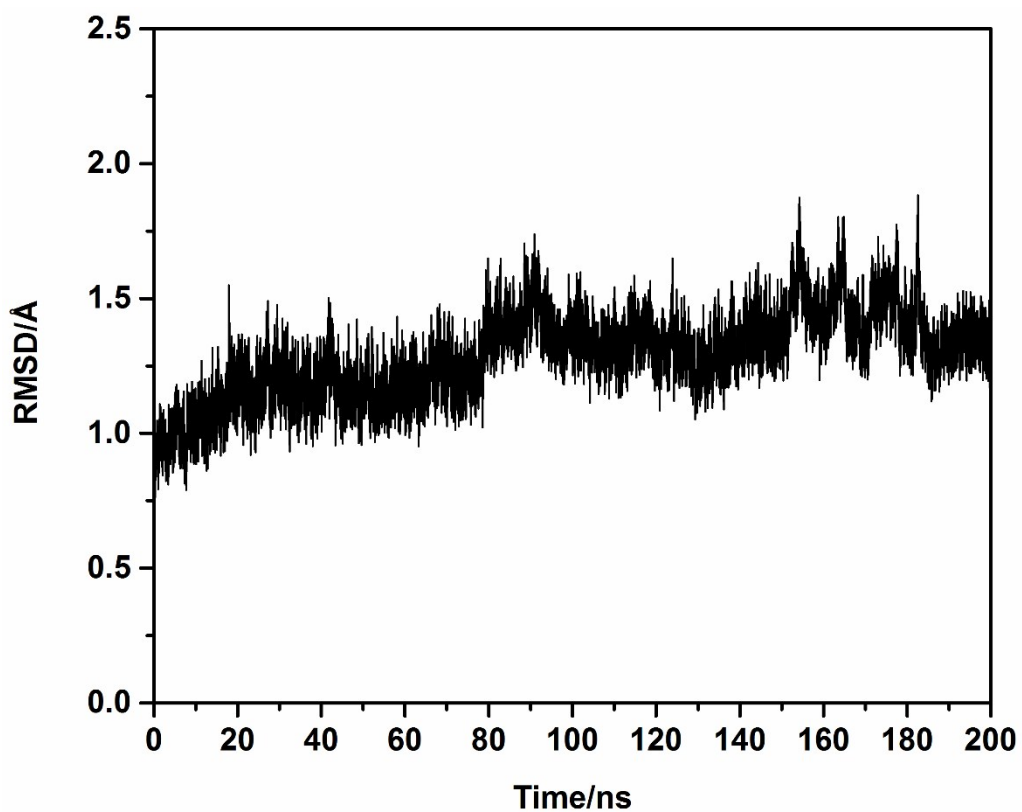


Fig. S1. Time evolution of RMSD (Å) for the alpha carbon atoms of the ZIKV protease in complex with the dipeptide inhibitor during MM MD simulation.

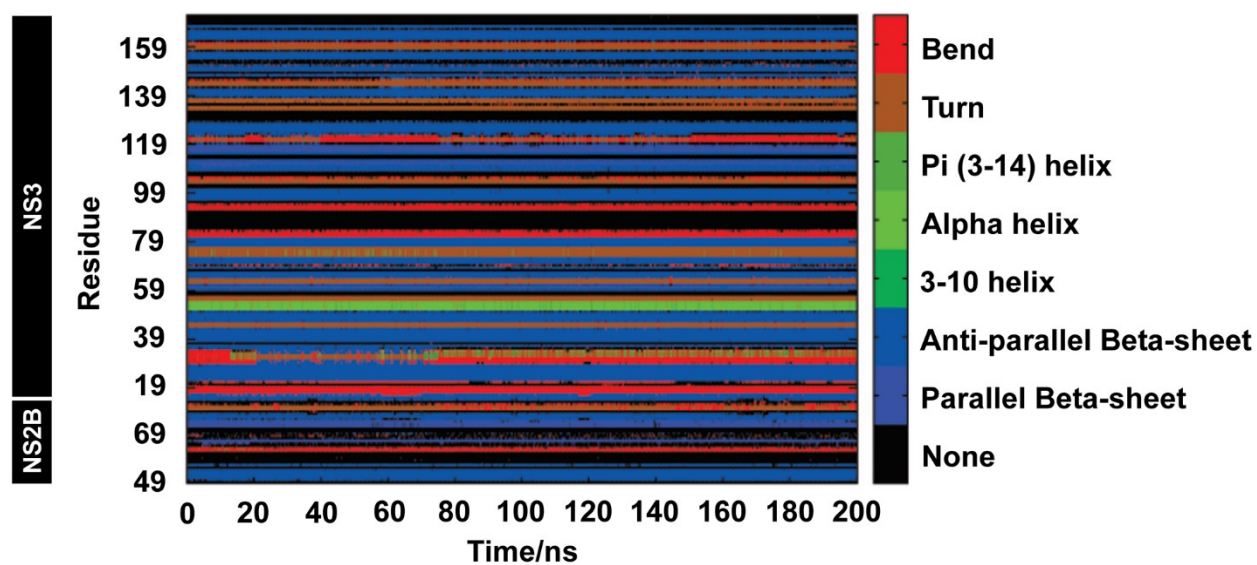


Fig. S2. DSSP plot of the secondary structure of the ZIKV protease with the dipeptide inhibitor bound during MM MD simulation.

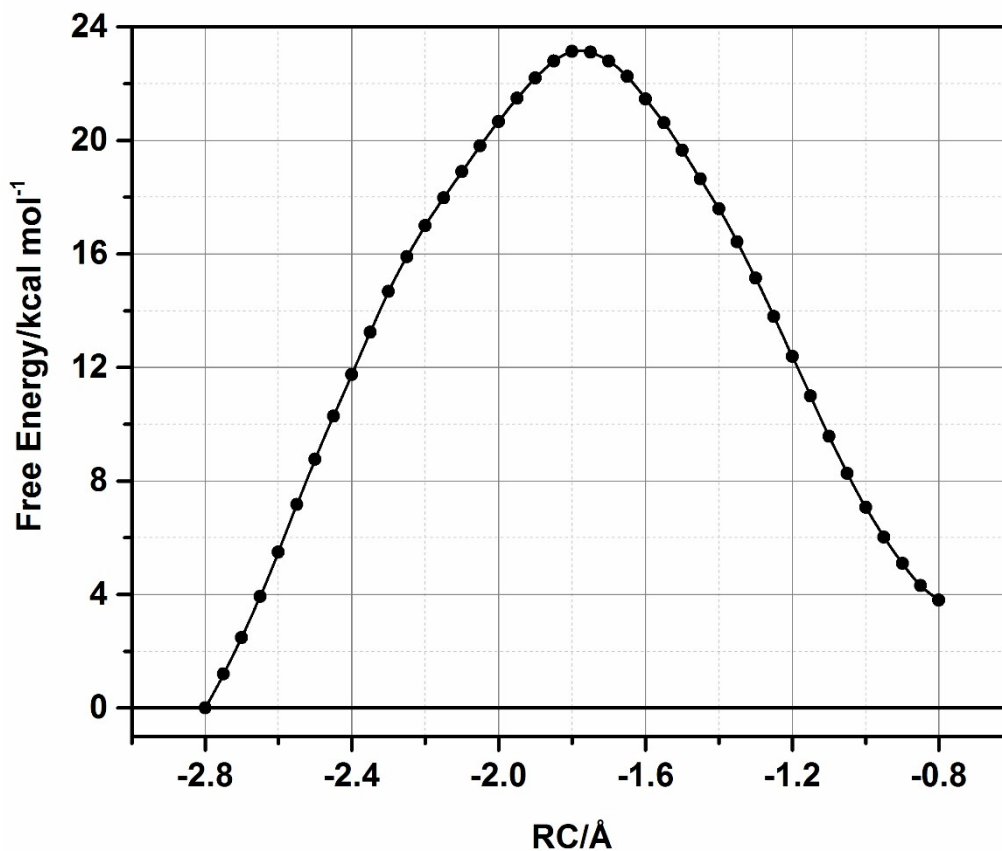


Fig. S3. Free-energy profile for the reaction of formation of the charged tetrahedral intermediate from the aldehyde (energy shown relative to the noncovalent Michaelis complex), using the combined reaction coordinates at the PM3/ff14SB level of QM/MM theory. This barrier is significantly higher than that calculated at the PDDG-PM3/ff14SB level (**Fig. 2** in the main text).

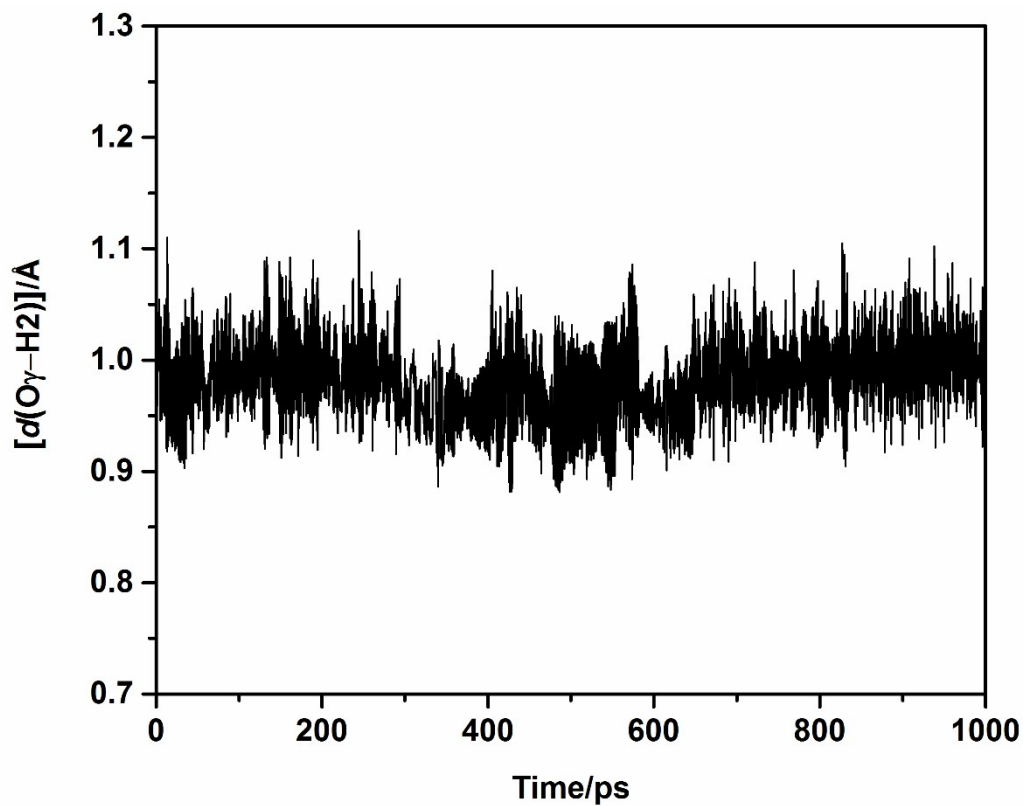


Fig. S4. Distance between oxygen atom (O γ) of the hemiacetal adduct and H₂_{H51} atom during 1 ns QM/MM (PDDG-PM3/ff14SB) MD simulation of the ZIKV protease bound with the dipeptide inhibitor. Proton transfer from H51 to form the hemiacetal has occurred spontaneously (see main text for discussion).

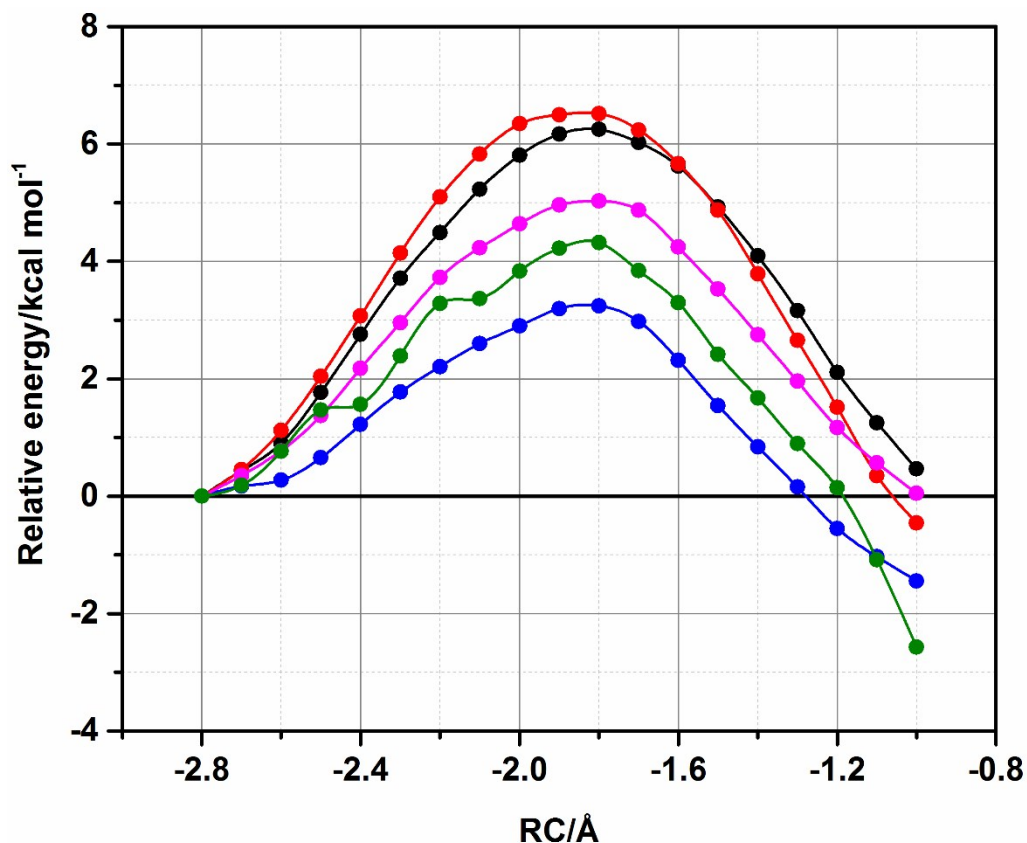


Fig. S5. Potential energy profiles for the reaction of formation of the charged tetrahedral intermediate calculated at the BH&HLYP-D3/6-31G(d)/ff14SB (black), BH&HLYP-D3/6-311+G(d)/ff14SB (red), MP2/(aug)-cc-pVTZ/ff14SB (blue), SCS-LMP2/(aug)-cc-pVTZ/ff14SB (magenta), and LCCSD(T)/(aug)-cc-pVTZ/ff14SB (green) QM/MM levels. All geometries were optimized at the BH&HLYP-D3/6-31G(d)/ff14SB level.

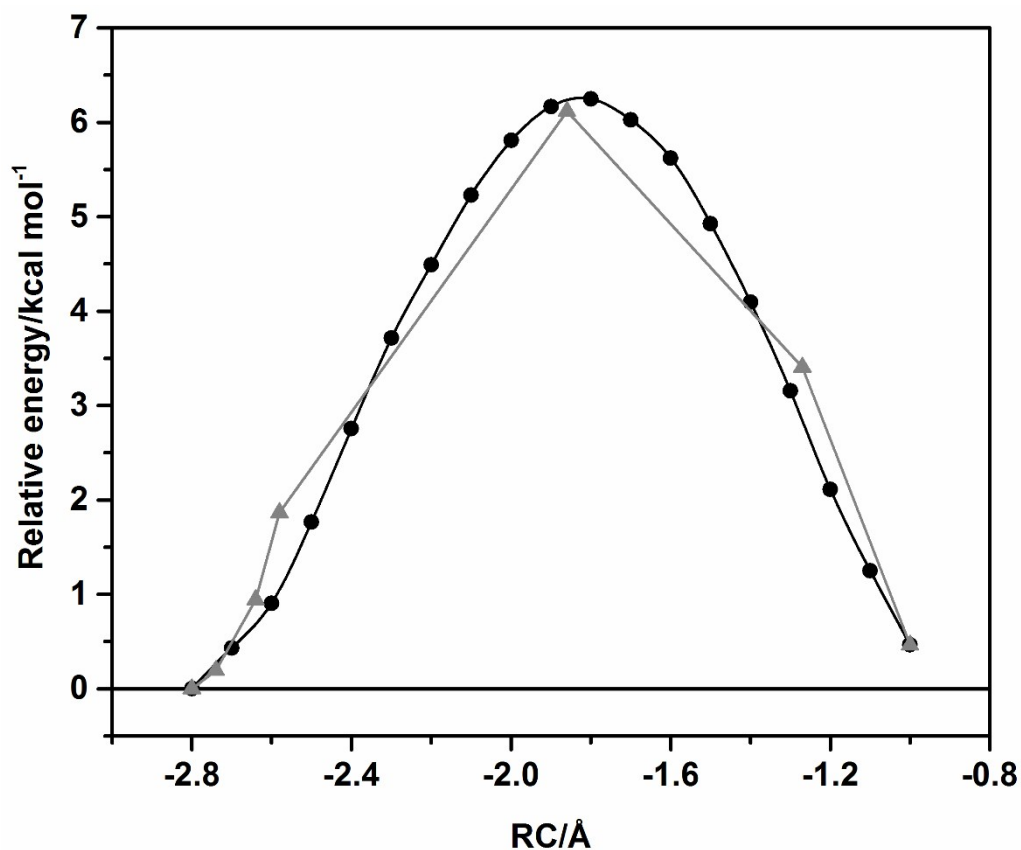


Fig. S6. Climbing image NEB profiles compared to adiabatic mapping (black circles, adiabatic mapping profile; grey triangles, CI-NEB profile from 7 starting images). Note that there is no reaction coordinate defined in the CI-NEB calculations; the data is plotted relative to the energy of the reactant and against the reaction coordinate to aid the comparison with the adiabatic mapping profile. All profiles are calculated at the BH&HLYP-D3/6-31G(d)/ff14SB level of theory and correspond to the reaction of formation of the tetrahedral adduct.

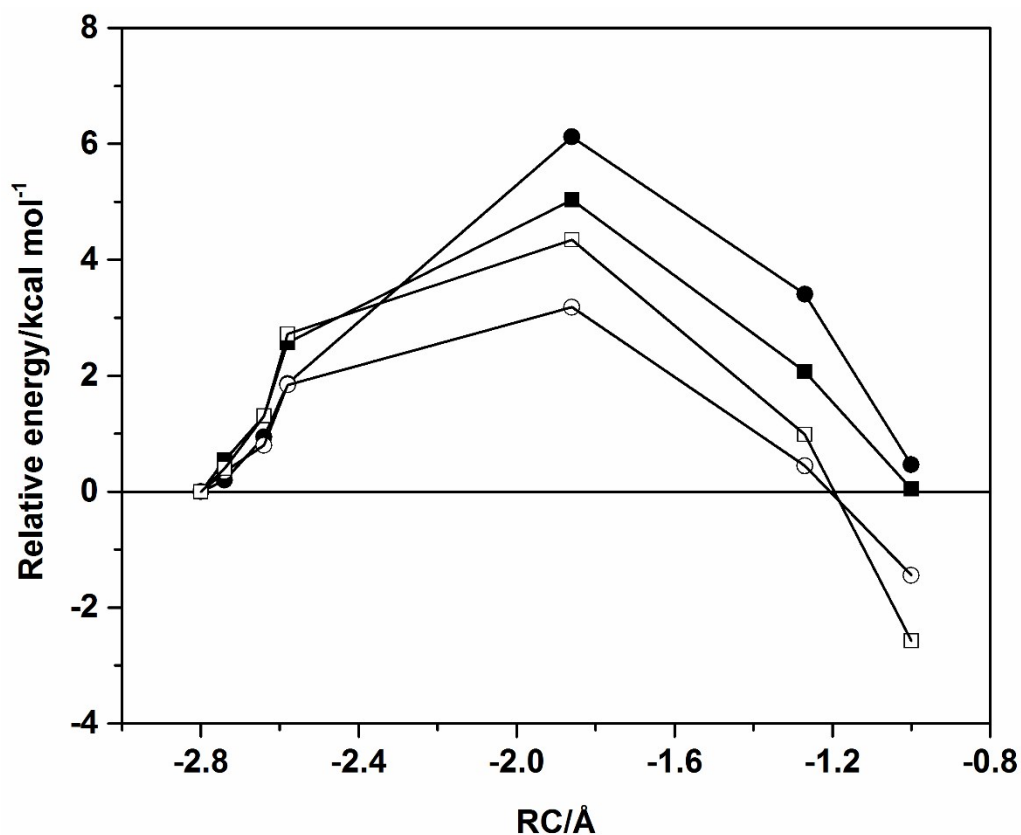


Fig. S7. Comparison of the potential energy profiles (relative to the reactant) for the reaction of formation of the charged tetrahedral intermediate at the BH&HLYP-D3/6-31G(d)/ff14SB (close circle), MP2/(aug)-cc-pVTZ/ff14SB (open circle), SCS-MP2/(aug)-cc-pVTZ/ff14SB (close square) and LCCSD(T)/(aug)-cc-pVTZ/ff14SB (open square) levels of theory (using the BH&HLYP-D3/6-31G(d)/ff14SB CI-NEB geometries). There is no reaction coordinate defined in the CI-NEB calculations; however, energies are plotted as a function of reaction coordinate for comparison.

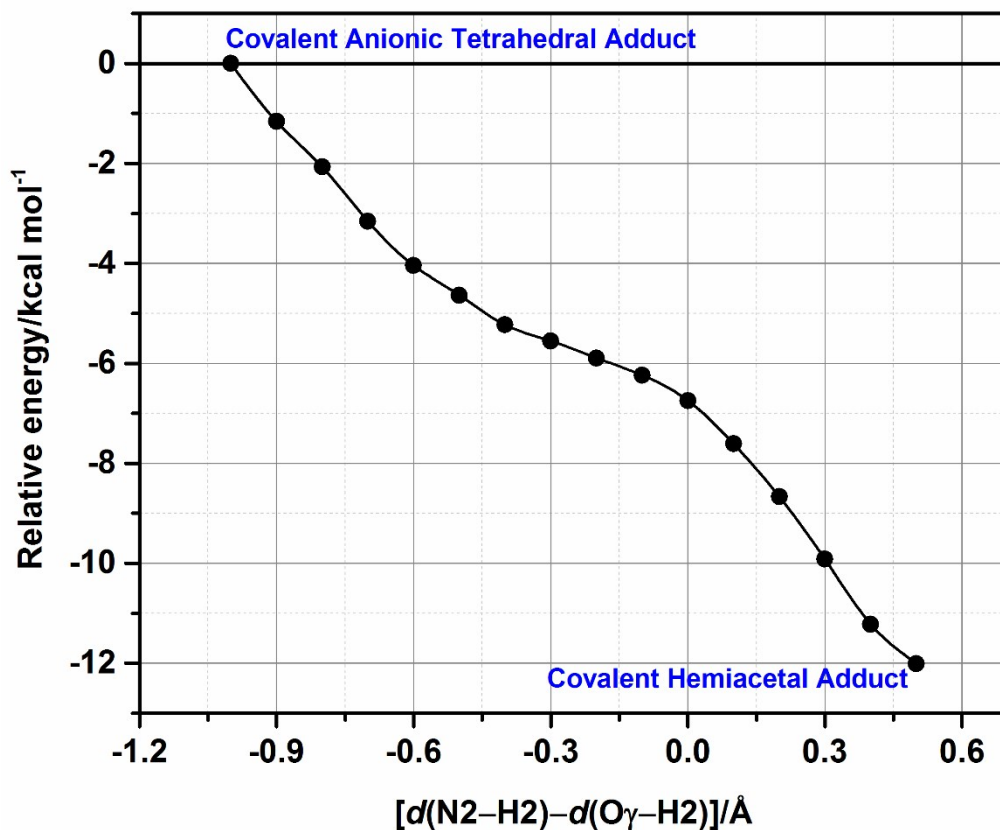


Fig. S8. Free-energy profile for the reaction of protonated hemiacetal adduct (relative to the reactant state, the charged tetrahedral intermediate) using reaction coordinate involving the direct proton transfer between H51 and oxygen atom of the tetrahedral adduct.

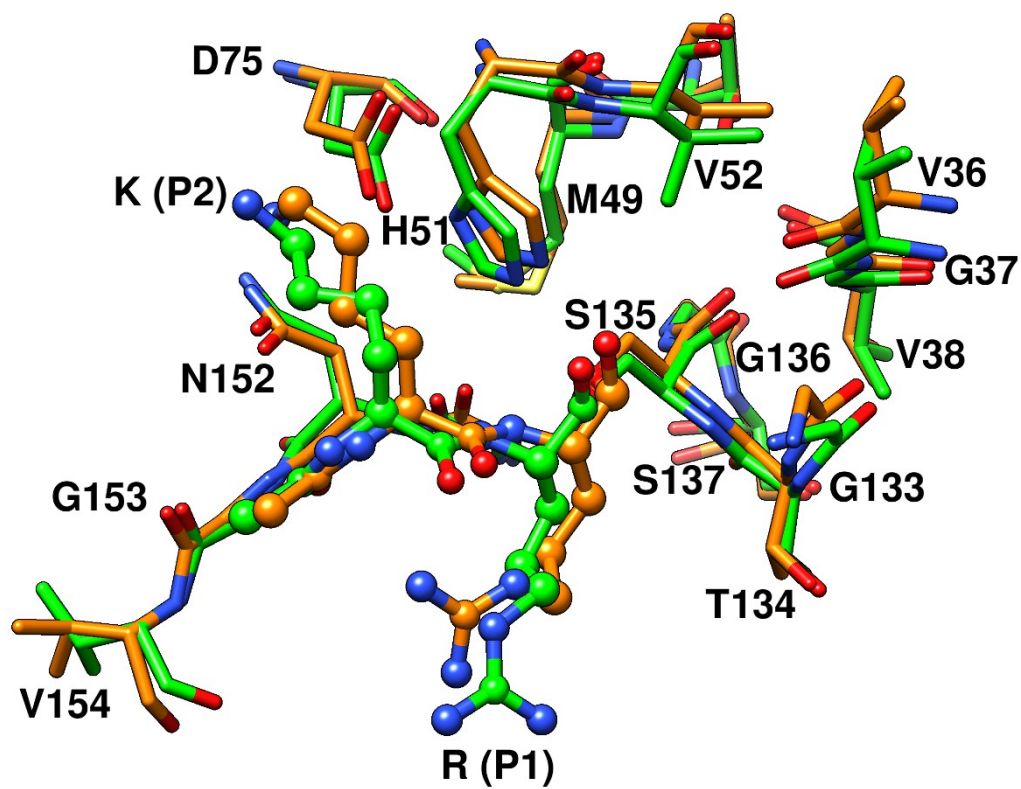


Fig. S9. Superposition of the DFT/MM (BH&HLYP-D3/6-31G(d)/ff14SB) structure of the hemiacetal (orange) with the crystal structure of the covalently bound inhibitor (green) on the active site of the ZIKV protease.

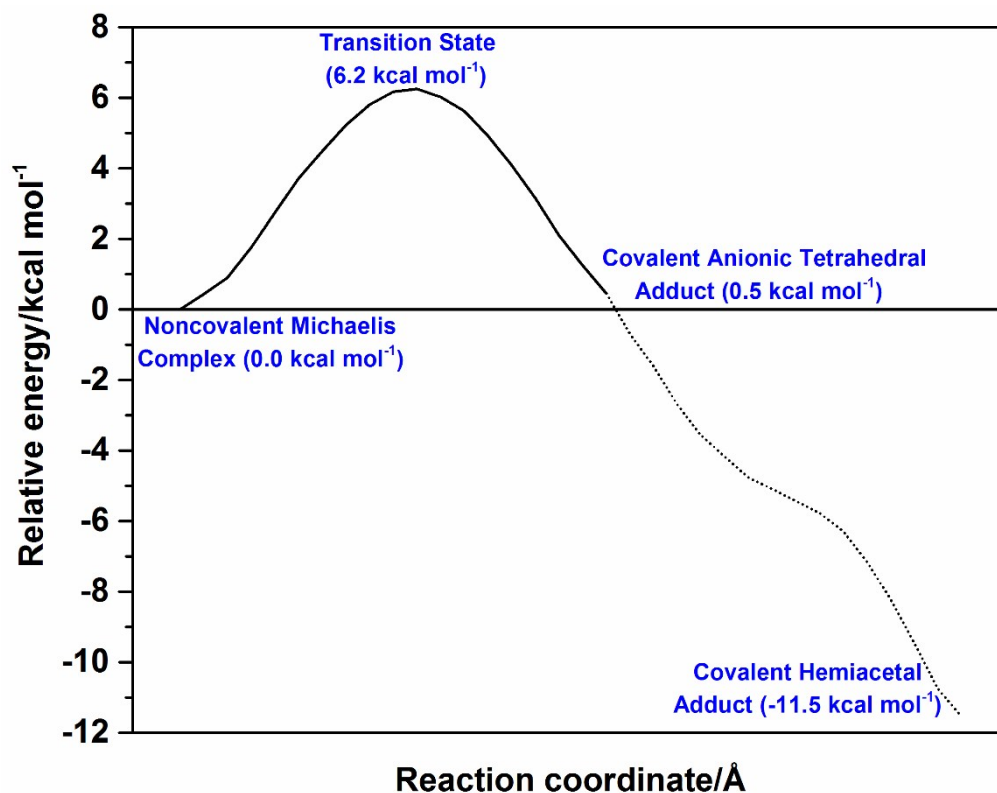


Fig. S10. Free-energy profiles for the reaction of formation of the charged tetrahedral intermediate (black line) and the protonated hemiacetal adduct (dotted line) (relative to the reactant state, the noncovalent Michaelis complex) calculated at the BH&HLYP-D3/6-31G(d)/ff14SB level of theory.